Food and Bioproducts Processing 144 (2024) 178–190

Contents lists available at ScienceDirect

Food and Bioproducts Processing

journal homepage: www.elsevier.com/locate/fbp

Effects of processing conditions on the release of sodium chloride from fat crystal 'shell' stabilised water-in-oil emulsions

R.L. Watson [a], I.T. Norton [a], B.R. Linter [b], A. Beri [b], F. Spyropoulos [a,*,1]

[a] School of Chemical Engineering, University of Birmingham, Edgbaston B15 2TT, United Kingdom
[b] PepsiCo International Ltd, 4 Leycroft Rd, Leicester LE4 1ET, United Kingdom

ARTICLE INFO

Keywords:
Water-in-Oil Emulsions
Pickering Stabilisation
Lipid Shells
Salt Release
Interfacial Rate Constants
Scraped Surface Heat Exchanger/Pin Stirrer

ABSTRACT

Over the last two decades, water-in-oil fat crystal stabilised Pickering emulsions have been increasingly studied for the controllable release of encapsulated (water-soluble) species. The stability inherent to Pickering emulsions has been shown to be enhanced by sintering to form an interfacial lipid 'shell' around the droplets, which improves the retention and prolongs the delivery of the enclosed species. Using a scraped surface heat exchanger/pin stirrer setup, the present work shows that processing conditions used to produced W/O emulsions with dispersed droplets enclosed in lipid shells, have a significant impact upon the subsequent release of NaCl enclosed within them. The best performing emulsion structure produced here is reported to retain about 98% of its initial salt load over a period of 100 days. NaCl release profiles were also used to calculate the interfacial rate constants for the transferal of salt across the lipid shells. Interfacial rate constants ranged from 5.5 to 3593.2×10^{-3} nm^2/s and were significantly (up to three orders of magnitude) lower than those reported in literature for similar systems. Analysis revealed that depending on the specific conditions employed, the processing environment can enhance or compromise lipid shell integrity. Overall, the current study offers significant direction in terms of the optimum processing requirements that are necessary to produce fat-continuous emulsion microstructures that can successfully regulate the release of NaCl, paving the way for the successful development of food formulations of controlled salt-perception.

1. Introduction

Since the early studies by (Ramsden, 1903) and (Pickering, 1907) on determining the influence of particles at interfaces and their role in stabilising emulsions, work in this area has continued to steadily grow (Lucassen-Reynders and Tempel, 1963). The main draw towards adopting a Pickering approach typically relates to achieving emulsion stabilisation that is more robust than that provided by low molecular weight emulsifiers (Aveyard et al., 2003). An increased interest in Pickering particle stabilised emulsions occurred with the development/creation of Pickering particles for applications in both the foods and pharmaceuticals sectors (Berton-Carabin and Schroën, 2015; Dickinson, 2020). In particular, the utilisation of fat crystals as Pickering particles in foods systems has been long appreciated;(Zafeiri et al., 2017) for example, fat crystals are the main stabilisation mechanism in margarine, a water-in-oil (W/O) emulsion. As a result, the use of fat crystal stabilisation in other food industry applications has attracted significant attention in recent years (Frasch-Melnik et al., 2010; Dickinson, 2012).

What is more, a combination of lipid components can have further synergistic effects in terms of fat crystal emulsion stabilisation. Some monoglycerides have been reported to displace other emulsifiers from interfaces during crystallisation to enable their hydrophilic ends to be located alongside the aqueous phase (Krog and Larsson, 1992). This surface-active behaviour has been shown to 'encourage' crystalline matter (e.g. triglyceride crystals) to associate with a water-in-oil interface and consequently assist in the formation of an interfacial 'shell' that shields the dispersed phase (Douaire et al., 2014; Ghosh and Rousseau, 2012). The sintering of fat crystals has been reported by Johansson *et al.* (Johansson and Bergenståhl, 1995) and is shown to be capable of producing a robust encapsulation system (Spyropoulos et al., 2011).

This type of approach has been further studied in the present work, for the encapsulation and subsequent release of sodium chloride (NaCl) from the dispersed phases of W/O emulsions. The encapsulation and

* Correspondence to: Fotis Spyropoulos University of Birmingham Birmingham, West Midlands United Kingdom.
E-mail address: f.spyropoulos@bham.ac.uk (F. Spyropoulos).
[1] ORCID: 0000-0002-0872-9328

https://doi.org/10.1016/j.fbp.2024.02.002
Received 21 November 2023; Received in revised form 17 January 2024; Accepted 9 February 2024
Available online 11 February 2024

release of sodium chloride is highly applicable to food systems, specifically with reference to salt reduction strategies. NaCl reduction is particularly beneficial from a health perspective, as high salt intake is known to raise blood pressure and thereby increase the risk of heart disease, stroke and other serious conditions (He and MacGregor, 2009). As consumption of processed foods is estimated to account for approximately 75% of our overall sodium intake, the food industry is at the forefront of research addressing the salt reduction challenge (Dötsch et al., 2009). While adapting consumer preferences in terms of saltiness by reducing sodium in products in small steps is accepted as probably the most promising strategy, this is a rather slow approach and more urgent interventions are required. As such, approaches that will allow the reformulation of existing processed foods so that they maintain the same perceived saltiness at lower sodium levels are urgently needed (Dötsch et al., 2009).

The hypothesis in the work presented here is that the localised concentration of flavour molecules bound to food microstructures, and their then more graduated release, can potentially reduce the levels of these molecules required (salt reduction), due to an increase in their (flavour) perception (Meiselman and Halpern, 1973; Noort et al., 2010). However, the encapsulation and release of small water-soluble molecules is a significant challenge in the creation of food microstructures. While trapping larger flavour molecules like sugars in food structures, in order to delay/modulate their release and perception, has been somewhat successfully achieved (e.g. by entrapping them in hydrocolloid gels), the high solubility and small size of salt ions can significantly hinder the effectiveness of such approaches (Holm et al., 2009).

W/O emulsions are excellent candidates for the entrapment of small ionic species and processes relevant to margarine production have been inspiring recent approaches for the successful manufacture and utilisation of such microstructures. Scraped Surface Heat Exchangers (SSHE) and Pin Stirrers (PS) have been used in the production of margarine for decades generating the fat crystals which stabilise the system (Anderson, 2005). A lab scale SSHE and PS Setup has enabled researchers to develop a better understanding of the processing phenomena occurring within these equipment, (Gabriele and Gels, 2011) as well as to develop new approaches for the production of aqueous systems dispersed in a solid fat matrix (di Bari et al., 2014; Norton et al., 2009).

The initial pass of a water/oil two-phase system through the SSHE generates crystals at the chilled equipment (inner) surface, which are then scrapped off and dispersed throughout the pre-emulsion generated. The formed crystals act as Pickering particles at the newly created W/O emulsion interfaces as well as nucleation sites for further (secondary) crystallisation to occur; both in the bulk/continuous oil phase and at the interface. The use of the PS unit then allows continued crystallisation at low temperatures, also increasing the presence of crystals at interfaces. The shear field imposed in the PS 'refines' the pre-emulsion and also acts to limit crystal network formation, reducing the viscosity of the resulting emulsion (Anderson, 2005). It should be noted however, that the application of shear to these systems can also serve to damage the formed interfacial crystal shells. This, in addition to the presence of any poorly encapsulated dispersed phase droplets, will result in the rapid release of actives. In the case of a small ionic load (e.g. NaCl), this is expected to result in the almost immediate release of the active from the system.

The current work aims to demonstrate the impact of processing conditions on the effective encapsulation of NaCl within sintered fat crystal 'shells' created with a lab-scale SSHE and PS assembly. More specifically, the flow rate and number of passes through the devices, the cooling temperature employed, and the uniformity and magnitude of the imposed shear, were all studied in terms of their effect on the emulsion microstructure generated as well as subsequently on its capacity to modulate the release of salt enclosed within it. To this end, it is demonstrated that these conditions outweigh the significance of the emulsion droplet size distribution in the successful encapsulation of NaCl.

2. Methods and materials

2.1. Materials

A combination of mono- and triglycerides were used for the preparation of the fat crystal stabilised emulsions in this work. This consisted of a 1:4 ratio of Dimodan P/PEL B Kosher (Danisco A/S, Grindsted, Denmark) and Tribehenin (Edenor® C22 85GS, Emery Oleochemicals GmbH), respectively. This ratio has been reported by Frasch-Melnik et al. (2010) to be successful in producing fat crystal stabilised W/O emulsions that are stable at temperatures up to 20°C. A higher melting point triglyceride (tribehenin) was selected in order to enhance the crystallisation driving force with the minimum reasonably accessible cooling temperatures using water. The higher melting point triglyceride was also envisaged to aid in reducing the effect of ambient temperatures on the stability of the encapsulation system. High oleic sunflower oil (Cargill) was used as the continuous phase solvent for the mono and triglycerides; the mono/triglyceride mixture was added at 2.5% of the continuous phase. Sodium Chloride (Food Grade (Table Salt), Sherman Chemicals Ltd., UK) was used to prepare 1 M salt solutions as the dispersed phase with double distilled water. All preparation was undertaken by weight and all the water (salt solution)-in-oil (W/O) emulsions prepared consisted of 30% dispersed phase (by weight). All materials were used as received with no further purification undertaken.

2.2. Processing equipment

In order to investigate the roles played by the residence time, cooling temperature and shear rate during processing on the emulsions, two different sets of Scraped Surface Heat Exchangers and Pin Stirrers were utilised. The SSHE and PS setup in which flow rate and number of passes (i.e. residence time), and temperature variations were studied shall be referred to as 'Setup 1'; this has been described in detail elsewhere (Frasch-Melnik, 2011; Norton and Fryer, 2012; di Bari, 2015). In brief and with regards to 'Setup 1', the used SSHE had a processing (internal) volume of approximately 25 ml, housing a 24×80 mm cylindrical stirrer equipped with two 70 mm scrapper blades (upon rotation of the stirrer, the centrifugal force pushes the blades out, causing them to come into contact with the internal wall of the vessel), while the used PS had a processing (internal) volume of approximately 170 ml, housing a 15×133 mm cylindrical stirrer equipped with sixteen 5×11 mm cylindrical pins (rotating pins); there are also an additional sixteen 5×11 mm cylindrical pins on the internal wall of the vessel (stationary pins) (Frasch-Melnik, 2011; di Bari, 2015). The SSHE and PS units in Setup 1 were operated at rotation rates of 1250 rpm and 1200 rpm respectively, where Table 1 shows the corresponding tip speeds. The complex flow and hence shear involved in both the SSHE and the PS prevent an equivalent shear rate being presented.

The work of Gabriele and Gels, (2011) on the flow regime and internal shear rates in the PS used in Setup 1 led to some improvements in the design of its internal geometry in order to eliminate/minimise the occurrence of stagnation zones. This resulted in a more efficient action of the applied shear, making this optimised setup ideal for investigating

Table 1
Tip speeds for SSHE and PS units. Setup 1 describes the constant speed setup used to investigate temperature and residence times, while Setup 2 describes the variable speed setup used to investigate high to low shear processing.

	Setup 1		Setup 2	
Rotation speed setting (rpm)	SSHE (m/s)	PS (m/s)	SSHE (m/s)	PS (m/s)
500	-	-	0.8	1.0
1250	2.0	2.3	2.0	2.4
2000	-	-	3.1	3.9

the effect of shear rate during emulsion processing. This optimised setup will henceforth be referred to as 'Setup 2', where rotation speeds were precisely controlled at 500, 1250 and 2000 rpm. The PS used in Setup 2 had the same number of pins as the Setup 1 unit, but its internal (processing) volume was slightly smaller as a result of removing what was confirmed to be a dead-zone (in terms of shear) at the top of the pin stirrer and near the unit's outlet.

2.3. Emulsion preparation

The continuous (oil) phase containing the mixture of mono and triglycerides was heated to a temperature of 90°C whilst stirring. 1 M NaCl was heated to ~50°C then added to the continuous phase and stirred while heating to 90°C, producing the primary emulsion. This primary emulsion was passed through the SSHE and PS units with a Masterflex L/S digital economy drive peristaltic pump (Cole Parmer, UK), using thick walled peristaltic tubing. Flow rates were investigated at 12, 25 and 50 ml/min. The primary emulsion was observed to have undergone some coalescence during the pumping process with a degree of phase separation occurring prior to reaching the SSHE unit. The high shear environment of the SSHE unit ensured that the emulsion was reformed *in situ* with appropriate proportions of both phases entering the unit throughout production. The removal of the high shear mixing phase conventionally used to prepare the primary emulsion (Frasch-Melnik et al., 2010) acted to reduce the complexity of the emulsion preparation process, thus improving the suitability for industrial scale up.

Both the SSHE and PS units were cooled to induce crystallisation and further process the emulsion at equal temperatures in both units with the temperature maintained by recirculated water chiller units. The effect of cooling temperature was investigated in Setup 1 at 5, 15 and 25°C, with emulsion temperatures at the inlet and outlets shown in Table 4 in the results section.

Emulsions were passed through the processing setup one or more times, before being collected/stored. For samples with a single pass this was all the processing undertaken. Samples reported to have been produced following two or more passes were (after each individual pass) collected and held briefly at room temperature prior to being repassed through the two-unit setup.

2.4. Emulsion droplet size measurements

Emulsion droplet size distributions were measured using laser diffraction via a Mastersizer 2000 (Malvern Instruments, UK). Droplet sizes given are based on the volume-surface weighted mean diameter, $D_{3,2}$.

2.5. Confocal microscopy

Confocal fluorescence micrographs of selected fat crystal stabilised W/O emulsions were obtained using a Leica TCS SP5 (Leica, Germany) with a 1 μM fluorescent tag concentration. Monopalmitin tagged with BODIPY™ (4,4-Difluoro-5,7-Dimethyl-4-Bora-3a,4a-Diaza-s-Indacene-3-Hexadecanoic Acid; Thermo Fisher Scientific) was added to the hot pre-emulsion a couple minutes prior to processing through the SSHE and PS units allowing sufficient time for an even distribution. This allows confocal fluorescence microscopy to show the location of the tagged fat crystals throughout the system, as a fraction of the crystals present. Microscopy was also used to confirm the absence of droplet aggregation in all W/O emulsion produced.

2.6. Release measurements

Release of Sodium Chloride from the dispersed phase was measured in order to monitor encapsulation stability and assess the degree of shell breakage; both these being precursors to droplet coalescence. W/O emulsion samples of 5 g were placed into 14 kDa molecular cut-off dialysis membrane tubing (Sigma Aldrich, UK) and sealed. The W/O sample containing tubing was then immersed into 100 g of double distilled water, which acted as the sink/acceptor phase (Simovic and Prestidge, 2007; Dowding et al., 2005; Washington, 1989). Small aliquots of the aqueous sink phase were taken at regular intervals, gently agitated and allowed to stand for five minutes to remove any concentration gradients present. Their conductivity was then measured and finally each sample was decanted back into the aqueous sink. Sample losses during the conductivity measurements were monitored and determined to be insignificant, leading to the assumption that the volume of the aqueous acceptor phase remains constant throughout the duration of the release experiments. For most systems, salt release was measured for up to 100 days. Potential 'failure' of the encapsulating shells was expected to result in the release of their saline aqueous content, which would collect at the bottom of the dialysis tubing and would thus be in direct contact (through the membrane) with the surrounding aqueous reservoir, allowing the transfer of NaCl. The validity of this approach was confirmed by initially studying W/O emulsions of poor encapsulation stability and observing complete salt release within a matter of 2–3 days. After complete release the dialysis tubing of these systems was observed and was found to consist of an upper oil layer (containing the fat crystals) and a lower saline aqueous layer (assumed to be) in osmotic equilibrium with the acceptor water phase.

2.7. Release profiles

Cumulative release (CR) profiles for NaCl are presented as a function of time *t*. CR data are expressed as percentages and are calculated as the fraction of the cumulative amount of NaCl released at time *t* (M_t) over that released at infinite time (M_0):

$$CR = \frac{M_t}{M_0} \times 100\% \tag{1}$$

where M_t is the total mass of active (NaCl) measured in the acceptor phase at time *t*, and M_0 is the amount of active entrapped within the emulsion droplets at time $t = 0$.

2.8. Release modelling

Two limiting models have been proposed to describe the release of an active contained within emulsion droplets (Washington and Evans, 1995; Guy et al., 1982). The first model suggests that release is primarily driven by the diffusion of the active through the core of the emulsion droplet and towards the interface. It has been shown (Washington and Evans, 1995) that in the absence of interfacial hindrance and at long times, active release can be approximated by:

$$\frac{M_t}{M_0} = 1 - \frac{6}{\pi^2}\exp\left(-\frac{\pi^2 D}{r^2}t\right) \tag{2}$$

or its linear form:

$$\ln\left(1 - \frac{M_t}{M_0}\right) = \ln\left(\frac{6}{\pi^2}\right) - \frac{\pi^2 D}{r^2}t \tag{3}$$

where M_t and M_0 retain their previous meanings as defined for Eq. 1, D is the diffusion coefficient of the active in the emulsion droplet, and *r* is the globule radius. On the other hand, the second model proposes that release is mainly dictated by the transfer of the active across the emulsion interface. When interfacial transport is the rate-limiting step, the following long-time approximation for the release of an active has been proposed (Washington and Evans, 1995):

$$\frac{M_t}{M_0} = 1 - \exp\left(\frac{-3k_1}{r^2}t\right) \tag{4}$$

where k_1 is the interfacial rate constant; all other symbols retain their

previous meaning. Eq. 4 can be rearranged to give:

$$\frac{r^2}{3}\ln\left(1-\frac{M_t}{M_0}\right) = -k_1 t \quad (5)$$

NaCl release from the W/O emulsions studied here is expected to be dominated by transferal of the active across the emulsion interface (lipid shells) and as such it should be fitted to the second of the two models. Fitting the NaCl data from the fastest releasing emulsion systems to Eq. (Lucassen-Reynders and Tempel, 1963) gives a diffusion coefficient of 4.5×10^{-18} m^2/s, which is extremely low to correspond to the diffusion of a small molecule through a liquid phase of relatively low viscosity. What is more, this value is significantly lower to the diffusion coefficient for NaCl within water as estimated using the Stoke-Einstein equation (8.9×10^{-10} m^2/s). As such, the diffusion-limited model is not applicable to describe the release behaviour observed in this study and instead NaCl data were fitted to the model assuming that overall transport of the active is controlled by the nature of the interfacial layer (Eq. (Berton--Carabin and Schroën, 2015)); best-fit parameters were used to calculate the interfacial rate constants k_1 for the discharge of NaCl from all studied W/O emulsions.

3. Results and discussion

The work presented here is organised into the three key processing variables under investigation, namely: *Residence Time* (i.e. flow rate and number of passes), *Cooling Temperature* and *Shear Rate*. In each case, the relevant droplet size distributions and NaCl release data are presented and analysed. Fig. 1 shows a confocal micrograph of a single pass W/O emulsion created at 1250 rpm with a flow rate of 25 ml/min and a cooling temperature set at 15°C; conditions representing a mid-range for the processing parameters investigated in this study (see Table 1). The green fluorescence highlights the fat crystal shells and the excess fat crystals at the interstices between them. The micrograph clearly shows that the majority of crystalline material is indeed associated with the water/oil interfaces of the emulsions and is supportive of the hypothesis on the existence of fat crystal 'shells' around the aqueous dispersed phase droplets. This microstructural characteristic was a typical feature in all emulsions produced throughout this study and thus demonstrates that the very approach of encapsulating NaCl within the aqueous dispersed droplets is successfully realised.

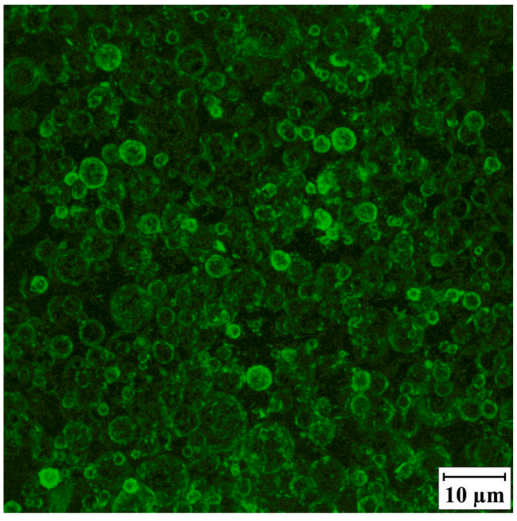

Fig. 1. Confocal Fluorescence Micrograph of a typical Fat Crystal Stabilised W/O emulsion produced in the present study.

3.1. The effect of residence time

3.1.1. The effect of liquid flow rate

The initial pass through the SSHE unit assists in the generation of fat crystals, which act as Pickering particles, stabilising the emulsion produced. The time in the PS unit allows further droplet size reduction and promotes adsorption of fat crystals at the newly created emulsion interfaces. With the aid of the cooling system (particularly in the PS unit), these fat crystal stabilised interfaces are then encouraged to transform into lipid shells, encasing the water droplets of the emulsion. The size (and size distributions) of the dispersed phase droplets and their corresponding NaCl release characteristics after a single and/or double pass through SSHE/PS Setup 1 at flow rates of 12, 25 and 50 ml/min are presented in Fig. 2 and Table 2.

The first pass data shown in Fig. 2A reveal a significant size difference between the systems produced at 12 ml/min and those at the 25 and 50 ml/min flow rates. Upon second pass through the SSHE/PS units (Fig. 2B), while the emulsion produced at the highest flow rate (50 ml/min) exhibited no changes to its first pass droplet size distribution, there is significant change to the droplet sizes obtained at 25 ml/min; the $D_{3,2}$ average diameter decreases from 104.1 to 23 µm, however even after a second pass through the SSHE/PS units, the emulsion still retains a small shoulder at the lower size range (around 5 µm). For the 12 ml/min flow rate, a double pass does not result in any significant droplet size change (with $D_{3,2}$ average sizes at 3.6 µm and 5.5 µm for the first and second passes, respectively), however it does cause a narrowing of the size distribution; span value reduces from 1.38 to 1.05 (Table 2).

The release profiles in Fig. 2C and D show a typical trend, usually exhibiting an initial rapid (in comparison) release, followed by a significantly reduced release rate (or even a plateau) for the remaining duration of the study. Although the 25 and 50 ml/min single pass systems had virtually identical size distributions (Fig. 2A), they exhibited significantly different release profiles, with the 50 ml/min system reaching a lower total NaCl release over the experimental period (~100 days). Conversely, after a second pass through the setup (i.e. increasing the residence time of the system in the processing environment of the SSHE/PS units), although the droplet size distributions of the emulsions produced at 25 and 50 ml/min differed significantly, their NaCl release profiles were very similar. Finally, the 12 ml/min sample showed a significant increase in release rate following a second pass through the SSHE/PS units, despite the relatively small change to its droplet size.

What might be initially perceived as a lack of correlation between emulsion droplet size and NaCl release rate, is obviously neglecting the contribution of the interfacial lipid shells. The NaCl cumulative release data (at longer times; $t \geq 10$ days) for all studied W/O emulsions were fitted to Eq. (Berton-Carabin and Schroën, 2015) (Fig. 2E and F); droplet radii were taken as half of the (previously obtained) corresponding $D_{3,2}$ values. The gradient of the produced linear fits (in most cases with $R^2 \geq 0.9$) is equal to $-k_1$; where k_1 is the interfacial rate constant. This process allows for the calculation of the rate constants for the transferal of NaCl across the W/O emulsion interface (Table 2), which can be used to assess the integrity of the lipid shells as a function of flow rate and number of passes.

The interfacial rate constants obtained range from 5.5 to 3593.2×10^{-3} nm^2/s (Table 2). The flow rate used in the production of the W/O emulsions appears to have a significant effect on the interfacial rate constant of the lipid shells created. Low flow rates (12 ml/min) provide lipid shells of much reduced permeability, compared to those formed at higher flow rates (25 and 50 ml/min). This clearly reflects the impact of a longer residence time (associated with the lower flow rates) and suggests that prolonged exposure of the microstructures to an environment that promotes crystallisation, results in further build-up of crystalline matter at the interface.

Extending this exposure by passing the structures through the SSHE/PS units (at the same flow rates) for a second time (pass 2), appears to have a varying effect in terms of promoting more robust lipid shells (i.e.

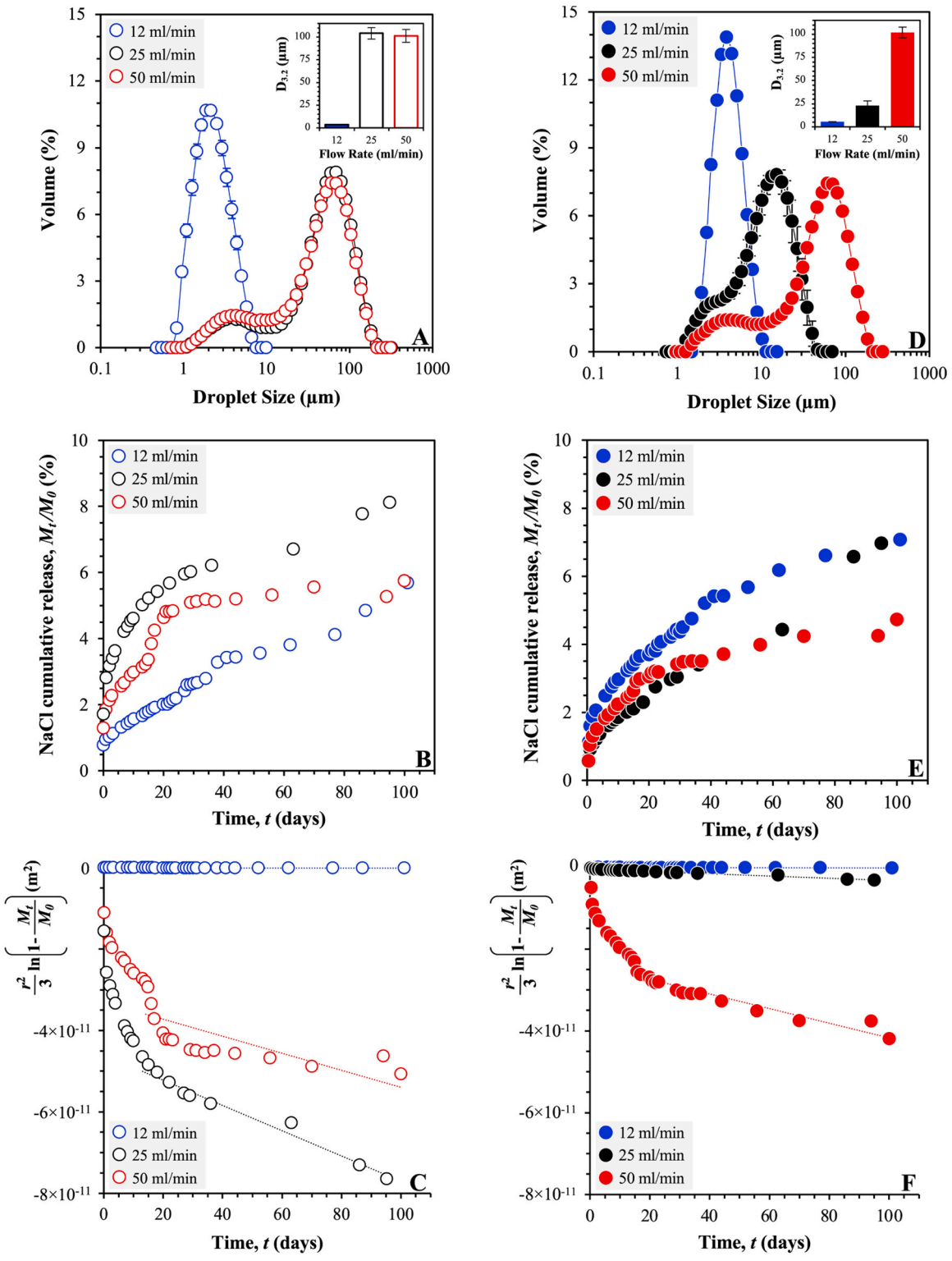

Fig. 2. **A** & **D**: Droplet size distributions of NaCl-containing (1 M in the aqueous dispersed phase) 30/70 W/O emulsions stabilised by a 1.75% (or 2.5% in the continuous phase) mono/triglyceride mixture (a 1:4 ratio of Dimodan and Tribehenin), as a function of flow rate and number of passes through the SSHE/PS units (Setup 1), operating at 1250 rpm and 5°C cooling; (**A**) single and (**D**) double pass data. **B** & **E**: NaCl cumulative release (%) from W/O emulsions (detail as above) as a function of flow rate (ml/min) and number of passes through the SSHE/PS units (detail as above); (**B**) single and (**E**) double pass data. **C** & **F**: First order fits to eq. (Berton-Carabin and Schroën, 2015) of data (for times $t \geq 10$ days) for the NaCl cumulative release from W/O emulsions (detail as above) as a function of flow rate (ml/min) and number of passes through the SSHE/PS units (detail as above); (**C**) single and (**F**) double pass data.

Table 2
Average droplet sizes (D3,2) and span values of NaCl-containing (1 M in the aqueous dispersed phase) 30/70 W/O emulsions stabilised by a 1.75% (or 2.5% in the continuous phase) mono/triglyceride mixture (a 1:4 ratio of Dimodan and Tribehenin), as a function of flow rate and number of passes through the SSHE/PS units (Setup 1), operating at 1250 rpm and 5°C cooling. Interfacial rate constants (k1) calculated by fitting the NaCl release from each of the tested W/O emulsions (see above) to Eq. (Berton-Carabin and Schroën, 2015), are also provided; SD: Standard Deviation.

	Flow Rate (ml/min)	$D_{3,2} \pm$ SD (μm)	span	$k_1 \pm$ SD $\times 10^{-3}$ (nm^2/s)	R^2
Pass 1	12	3.6 ± 0.2	1.38	5.5 ± 0.4	0.969
	25	104.1 ± 6.3	2.08	3593.2 ± 494.1	0.978
	50	101.3 ± 7.0	2.16	2422.6 ± 1028.9	0.517
Pass 2	12	5.5 ± 0.1	1.05	15.3 ± 2.5	0.937
	25	23.0 ± 5.0	1.92	313.5 ± 23.2	0.986
	50	101.9 ± 5.8	2.19	2070.6 ± 353.9	0.918

lower interfacial rate constant values). When the second pass is accompanied by a significant droplet size reduction (as is the case for the 25 ml/min flow rate), then the decrease in the obtained interfacial rate constant values clearly suggests the creation of more impermeable interfacial lipid shells. This is hypothesised to be a result of the associated increase in interfacial area, which encourages further deposition/adsorption of crystalline matter at the interface. When the second pass through the SSHE/PS units does not cause a change to the droplet size of the W/O emulsion (generated during the first pass), then interfacial rate constants either remain largely unaffected (as for the 12 ml/min flow rate) or are more modestly reduced (as for the 50 ml/min flow rate). In the first case (flow rate of 12 ml/min), the longer residence time (per pass) ensures that an optimum lipid shell has been generated upon first pass through the SSHE/PS units, and further exposure to the same environment (over the same timescales/residence time) does not offer any further improvement in terms of enhancing lipid shell integrity. In the second case (flow rate of 50 ml/min), the shorter residence time (per pass) is not expected to have an impact on lipid shell integrity, as it hardly affects emulsion droplet sizes to begin with. Here, the shorter exposure to the processing environment would not be expected to promote the adsorption of further crystalline matter (on average, interfacial area does not change), and the small decrease to the interfacial rate constant is then potentially due to further deposition of crystals at the (already formed) interfacial lipid shells.

The reporting of interfacial rate constants in systems that are similar to those studied here is very scarce in literature. Interfacial rate constants are typically provided for the release of hydrophobic actives from O/W emulsions. Spyropoulos et al. (2020) reported interfacial rate constants (k_1) for the release of dimethyl phthalate (DMP) from O/W emulsions stabilised by different species; ranging from low molecular weight surfactants and protein polyelectrolytes, to biopolymer complexes and even solid particles. The study calculated k_1 values in the range of 20–600 nm^2/s, with only the lower end values being comparable to (the higher end of) those presented here. Another study on the release of dibutyl-phthalate (DBP) from O/W emulsions stabilised by either hydrophilic or hydrophobic silica nanoparticles reported (only for systems stabilised by hydrophobic silica; Aerosil® R974) very low k_1 values; 0.3 and 0.05 nm^2/s, at NaCl concentrations of 10^{-3} and 10^{-1} M, respectively (Simovic and Prestidge, 2007).

In a study that is much more related to the systems investigated here, Yow and Routh (2009) considered the release of a hydrophilic dye (fluorescein) from water-in-oil (W/O) colloidosomes, formed using 180 nm latex particles, which were subsequently sintered to form W/O microcapsules; the size of the W/O colloidosomes was reported to be ~3.8 μm, while the subsequently formed W/O microcapsules were slightly smaller. The authors report dye-shell diffusion coefficients within the range of 0.6–11.1$\times 10^{-17}$ m^2/s (i.e. 6–111 nm^2/s), with the lower end of these values corresponding to structures that were sintered for 60 min. Despite utilising polymeric and not lipid species, there are some clear parallels between the systems studied by Yow and Ruth (Yow and Routh, 2009) and those reported here. The higher shell diffusion coefficients reported in the former could be due to the different nature of the interfacial shells created, but also because of lower shell thicknesses, as the authors hypothesise that a single layer of polymeric particles resides at the interfaces of the initially formed W/O colloidosomes.

3.1.2. The effect of multiple passes (at a fixed flow rate)

The W/O emulsion produced using a flow rate of 25 ml/min exhibited the greatest change, following a second pass through SSHE/PS units, in terms of both its droplet size distribution as well as its interfacial rate constant (see previous section). As such, this specific system was chosen to investigate the effect of multiple passes on the W/O emulsion microstructures and their interfacial lipid shells. The size distributions of the W/O emulsion droplets generated after each pass and their corresponding NaCl release characteristics are presented in Figs. 3A and 3B. In each case, the corresponding average droplet sizes ($D_{3,2}$), span values and interfacial rate constants (k_1) are presented in (Table 3).

Similarly to the effect of multiple passes on droplet size, NaCl release is progressively restricted upon each processing passage through the devices; a decrease in both the rate and overall amount of salt released from the emulsions is apparent. The hindrance to NaCl release is more pronounced for the initial passes (up to 3 passes), with further processing through the SSHE/PS units having a more moderate impact on salt expulsion. This is further confirmed by the values of the calculated interfacial rate constants; k_1 decreases by two orders of magnitude from the first to the third pass, beyond which it is only marginally reduced.

These findings align with the previous hypothesis that longer residence times (introduced by repeated passes through a fixed processing set-up that promotes further crystallisation), will significantly reinforce the integrity of the formed interfacial lipid shells, only if accompanied by a droplet size reduction (i.e. increase in interfacial area) which in turn encourages the build-up of additional crystalline matter around the emulsion droplets. If that is not the case (emulsion droplet sizes upon further processing passes are not reduced), any gains in terms of lipid shell fortification and NaCl release regulation will be much more moderate to almost insignificant.

3.2. The effect of cooling temperature

The operation temperature of the cooling jackets (surfaces) on the SSHE and PS units for Setup 1, was varied from 5°C to 25°C in order to investigate the impact on emulsion droplet size. An increase in the jacket temperature of the units, decreases both the extent and rate of crystallisation phenomena during processing, by reducing the magnitude of the induced cooling to the emulsion; i.e. the crystallisation driving force. The set jacket temperature however does not equate to the temperature of the emulsion, as the level of cooling conveyed to the emulsion is also a function of mixing (rotation speed) and residence time (flow rate/number of passes) in the unit. For this reason, emulsion temperatures at the inlet and outlet of the SSHE and outlet of the PS units (in Setup 1) were measured during operation and are presented in Table 4. Regardless of the cooling jacket temperatures tested, it is worth noting that the temperatures of all emulsions exiting either of the SSHE or PS units of the processing setup (i.e. the SSHE and PS Outlet temperatures in Table 4) were below the crystallisation temperature for the pure lipid mixture utilised throughout this study (Dimodan:Tribehenin at a mass ratio of 1:4); upon cooling the lipid mixture from 100°C at a rate of 10 °C/min, crystallisation starts at 77°C and concludes at 60°C, with no further crystallisation events below this temperature.

The droplet size distributions of the W/O emulsions produced using Setup 1 (operating at 1250 rpm and 25 ml/min) as a function of cooling temperature and number of passes are presented in Fig. 4A and D; first

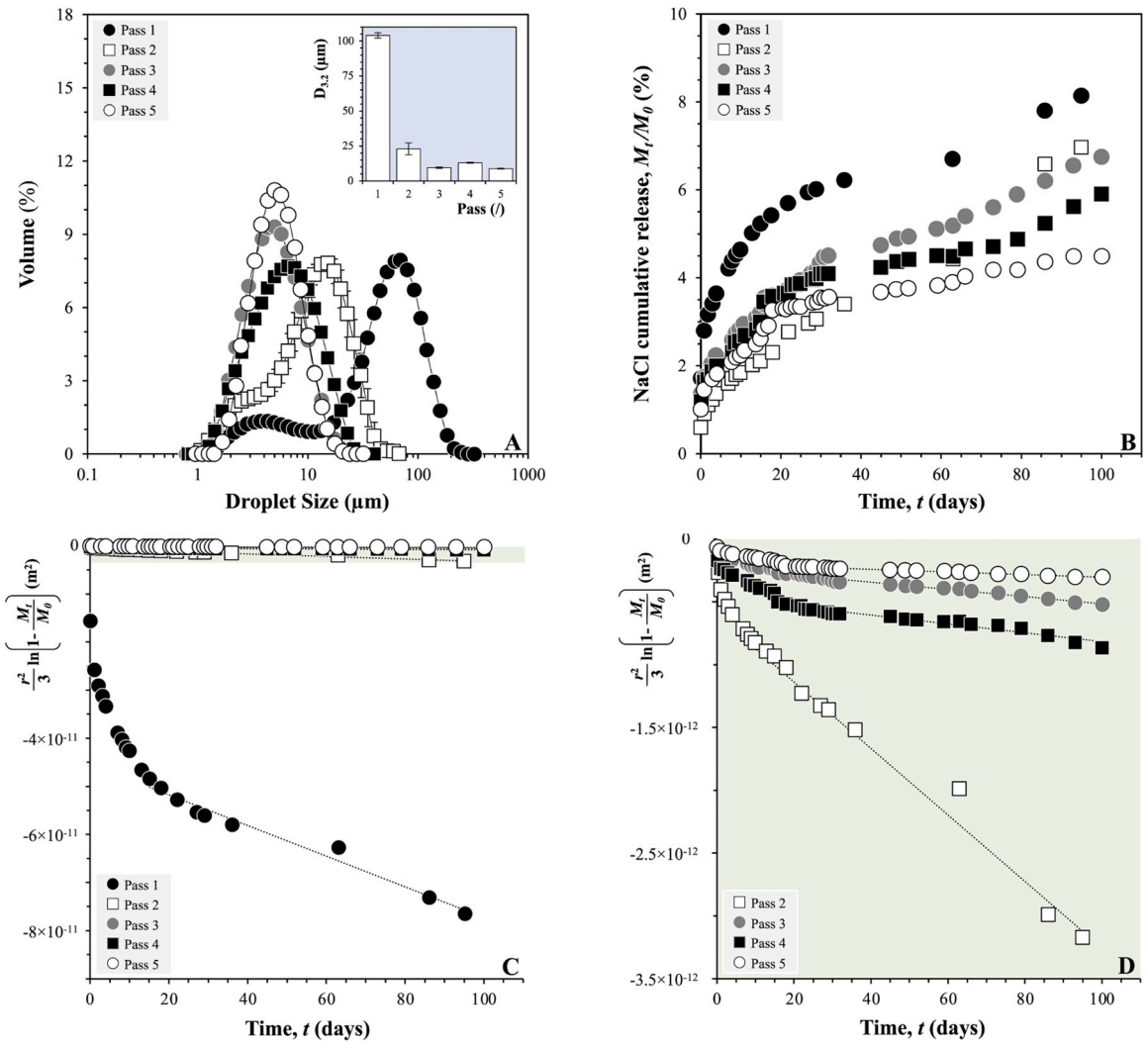

Fig. 3. A: Droplet size distributions of NaCl-containing (1 M in the aqueous dispersed phase) 30/70 W/O emulsions stabilised by a 1.75% (or 2.5% in the continuous phase) mono/triglyceride mixture (a 1:4 ratio of Dimodan and Tribehenin), as a function of number of passes through the SSHE/PS units (Setup 1), operating at 1250 rpm, 25 ml/min and 5°C cooling. B: NaCl cumulative release (%) from W/O emulsions (detail as above) as a function of number of passes through the SSHE/PS units (detail as above). C: First order fits to eq. (Berton-Carabin and Schroën, 2015) of data (for times $t \geq 10$ days) for the NaCl cumulative release from W/O emulsions (detail as above) as a function of number of passes through the SSHE/PS units (detail as above). D: Same as C, but providing better data visualisation for systems corresponding to 2 passes through the SSHE/PS units and above; graph area in D is equivalent to the shaded area in C.

Table 3
Average droplet sizes ($D_{3,2}$) and span values of NaCl-containing (1 M in the aqueous dispersed phase) 30/70 W/O emulsions stabilised by a 1.75% (or 2.5% in the continuous phase) mono/triglyceride mixture (a 1:4 ratio of Dimodan and Tribehenin), as a function of number of passes through the SSHE/PS units (Setup 1), operating at 1250 rpm, 25 ml/min and 5°C cooling. Interfacial rate constants (k_1) calculated by fitting the NaCl release from each of the tested W/O emulsions (see above) to Eq. (Berton-Carabin and Schroën, 2015), are also provided; SD: Standard Deviation.

Number of passes (/)	$D_{3,2} \pm$ SD (μm)	span	$k_1 \pm$ SD $\times 10^{-3}$ (nm^2/s)	R^2
1	104.1 ± 6.3	2.08	3593.2 ± 536.0	0.977
2	23.0 ± 5.0	1.92	313.5 ± 23.2	0.986
3	9.5 ± 0.6	1.55	35.2 ± 2.1	0.983
4	13.1 ± 0.4	1.85	46.5 ± 4.9	0.896
5	8.9 ± 0.3	1.31	15.4 ± 0.9	0.855

Table 4
Cooling jacket temperature settings for Setup 1 SSHE and PS units (operating at 1250 rpm and 25 ml/min), and corresponding measured temperatures at the inlet and outlet of the SSHE unit and outlet of the PS unit, as a function of passes through Setup 1. Absolute errors in temperature of ±0.3°C.

	Temperature (°C)			
	Cooling Jacket	SSHE Inlet	SSHE Outlet	PS Outlet
Pass 1	5	79.7	14.5	10.0
Pass 2		18.5	15.0	10.2
Pass 1	15	77.3	21.5	17.5
Pass 2		22.4	20.7	17.8
Pass 1	25	74.2	26.0	26.2
Pass 2		25.6	26.6	25.9

and second pass, respectively. The corresponding average droplet sizes ($D_{3,2}$) and span values for each formed emulsion are provided in Table 5. Upon first passage through both devices, all three cooling temperatures resulted in W/O emulsions with relatively large bimodal distributions, with the formulation produced at 15°C displaying the lowest average droplet size; 48 μm. Following a second pass, the droplet sizes of W/O emulsions produced using 5°C or 15°C cooling, were both reduced (giving $D_{3,2}$ values of 23 and 7.3 μm, respectively), however emulsions formed at 25°C appeared to increase in size (to a $D_{3,2}$ value of 99.6 μm). It is worth noting that despite the reduction in droplet size, the W/O

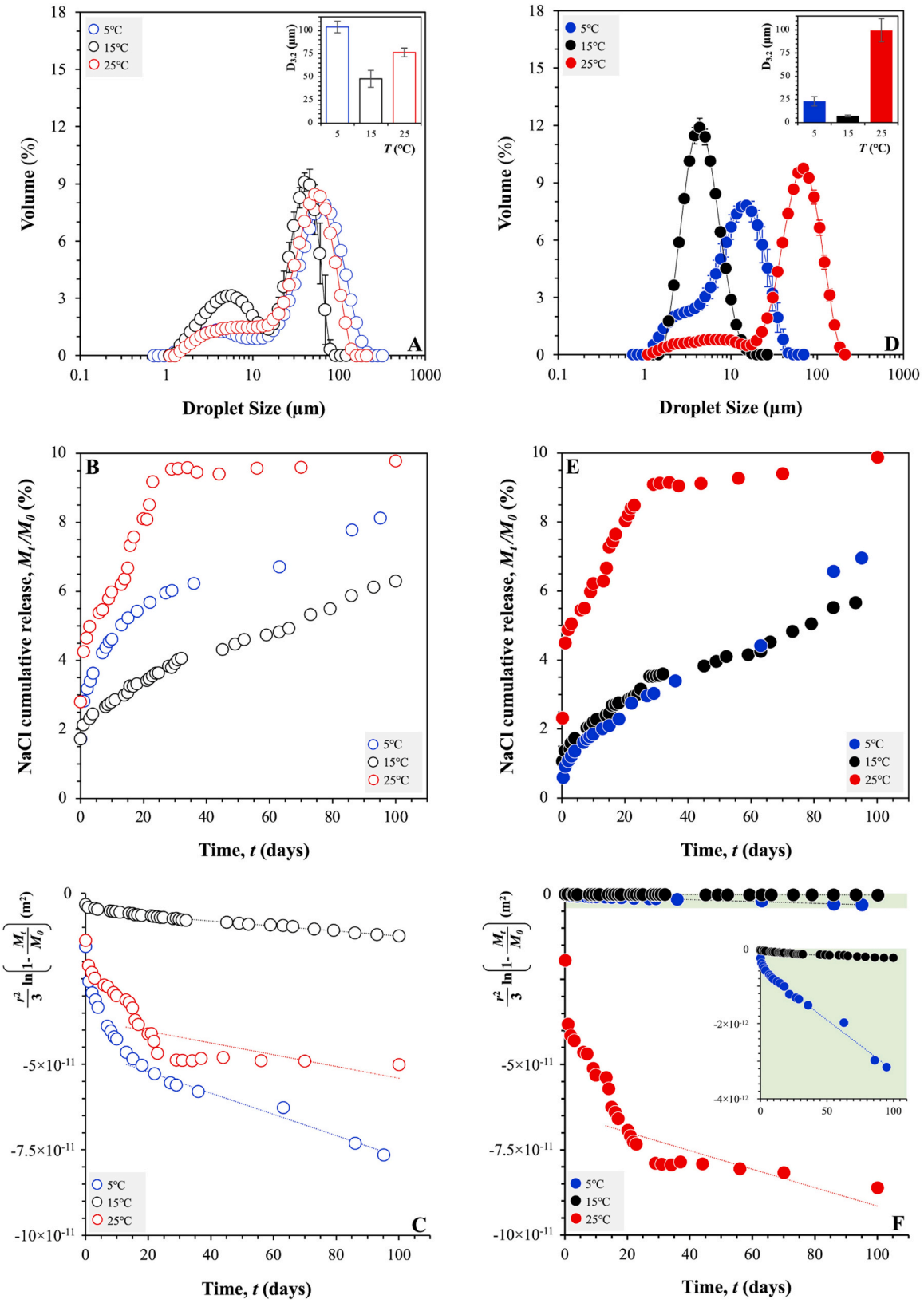

Fig. 4. Droplet size distributions of NaCl-containing (1 M in the aqueous dispersed phase) 30/70 W/O emulsions stabilised by a 1.75% (or 2.5% in the continuous phase) mono/triglyceride mixture (a 1:4 ratio of Dimodan and Tribehenin), as a function of cooling temperature and number of passes through the SSHE/PS units (Setup 1), operating at 1250 rpm and 25 ml/min; (A) single and (D) double pass data. B & E: NaCl cumulative release (%) from W/O emulsions (detail as above) as a function of cooling temperature and number of passes through the SSHE/PS units (detail as above); (B) single and (E) double pass data. C & F: First order fits to eq. (Berton-Carabin and Schroën, 2015) of data (for times $t \geq 10$ days) for the NaCl cumulative release from W/O emulsions (detail as above) as a function of cooling temperature and number of passes through the SSHE/PS units (detail as above); (C) single and (F) double pass data. The graph area of the inset plot in F is equivalent to the shaded area in the main graph.

emulsions produced at 5°C continue to display a bimodal distribution, while those formed at 15°C now (upon a second processing pass) exhibit a single size distribution peak. What is more, the average droplet sizes achieved at 15°C here (25 ml/min), are similar to those reported earlier at 5°C but for higher residence times; either after a second pass at a lower flow rate (12 ml/min; see Fig. 2 and Table 2) or after multiple passes at the same flow rate (25 ml/min; see Fig. 3 and Table 3).

The smaller droplet sizes produced after two passes at 15°C indicate that there may have been an element of overcooling for the systems formed at 5°C. A high degree of supercooling could have potentially led to the generation of larger fat crystals due to more rapid crystallisation and competing primary and secondary nucleation at existing crystal surfaces.(Basso et al., 2010) Larger crystals would in turn hinder the reduction in droplet size that can be achieved, as in this case the resulting greater interfacial area and curvature would require smaller crystals to enable complete surface coverage and thus effective stabilisation. Conversely, the droplet size data obtained for the W/O emulsions produced at 25°C suggest that the reduced cooling potential (provided in this case) does not deliver the crystal population required for interfacial stabilisation. As a result, droplet coalescence events during processing are more prevalent, leading to higher droplet sizes after the first pass through the SSHE and PS units for Setup 1 (Fig. 4 and Table 5). Allowing the formulation to re-enter the same processing environment for a second time, exacerbates such (coalescence) events, thus leading to further increases to the obtained droplet sizes. The overall behaviour presented here, also aligns well with the calculated span values for the emulsions (Table 5).

The impact of the cooling temperature on salt release from the produced W/O emulsions is shown in Fig. 4B and E. The data suggest a significant cooling temperature dependence, with faster and higher overall salt release being particularly notable at 25°C. The rapid initial release of NaCl at 25°C (in comparison to the other temperatures studied) indicates that there was a greater proportion of damaged or weak shells being formed around emulsion droplets manufactured at this temperature. The NaCl release performance exhibited by the emulsions formed at 25°C is preserved even after a second pass of these structures through the processing environment in Setup 1. Emulsion production at 15°C (first pass) resulted in the lowest (initial) salt release rates and overall released salt content. A second passage through the SSHE and PS units however brought the salt release rates of the W/O emulsions produced at 5°C and 15°C closer together, despite the difference in average droplet sizes between the two systems.

Interfacial rate constants for the transfer of NaCl across the W/O emulsion lipid shell interface, as a function of the cooling temperature used, are presented in Table 5; calculated k_1 values range from 19.5 to 3593.2×10^{-3} nm^2/s. The effect of cooling temperature on the capacity of the formed lipid shell to impede the migration of NaCl is significant.

Table 5
Average droplet sizes (D3,2) and span values of NaCl-containing (1 M in the aqueous dispersed phase) 30/70 W/O emulsions stabilised by a 1.75% (or 2.5% in the continuous phase) mono/triglyceride mixture (a 1:4 ratio of Dimodan and Tribehenin), as a function of cooling temperature and number of passes through the SSHE/PS units (Setup 1), operating at 1250 rpm and 25 ml/min. Interfacial rate constants (k1) calculated by fitting the NaCl release from each of the tested W/O emulsions (see above) to Eq. (Berton-Carabin and Schroën, 2015), are also provided; SD: Standard Deviation.

	Temperature (°C)	$D_{3,2}$ ± SD (μm)	span	k_1± SD × 10^{-3} (nm^2/s)	R^2
Pass 1	5	104.1 ± 6.3	2.08	3593.2 ± 536.0	0.977
	15	48.0 ± 9.1	1.85	847.3 ± 44.9	0.988
	25	76.4 ± 4.7	1.92	1986.2 ± 389.3	0.458
Pass 2	5	23.0 ± 5.0	1.92	313.5 ± 28.4	0.986
	15	7.3 ± 0.9	1.25	19.5 ± 1.7	0.970
	25	99.6 ± 12.5	1.77	3138.3 ± 867.9	0.615

W/O emulsions produced (single pass) at 15°C appear to give the more robust lipid shells, while those formed at 5°C exhibit the lowest levels of interfacial hindrance. A second passage through the SSHE/PS units reduces the permeability of the previously formed lipid shells (as suggested earlier) only for systems produced at cooling temperatures of either 5°C or 15°C. On the contrary, the robustness of the interfacial lipid layers formed around the W/O emulsions produced at 25°C appears to be further compromised following a second processing pass; in agreement to what was earlier suggested by the droplet size data. It should be noted that the coefficients of determination (R^2) for the linear fits performed in the calculation of k_1 for the systems produced at 25°C (single and double passes), are poor and therefore confidence in the determined interfacial rate constant values is low. However, this also suggests that these systems do not entirely behave according to the inherent assumptions in the used model; i.e. structures with a coherent interfacial layer that dominates the release of entrapped species. Similarly to what was suggested upon consideration of the effect of cooling rate on the droplet sizes of the emulsions, the interfacial rate constants achieved at 15°C here (25 ml/min), are similar to those reported earlier at 5°C but for higher residence times; either after a single pass at a lower flow rate (12 ml/min; see Table 2) or after multiple passes at the same flow rate (25 ml/min; see Table 3).

3.3. The effect of shear

3.3.1. The effect of shear uniformity

The SSHE and PS setup used in this part of the work to study the influence of shear rate (Setup 2) utilises a pin stirrer unit that has been shown to provide a more uniform shear rate environment (in comparison to that of Setup 1), by diminishing the existence (and thus the impact) of stagnation zones (Gabriele and Gels, 2011). As a result, Setup 2 produces W/O emulsions with a significantly smaller average droplet size (compared to those delivered by Setup 1), even upon a first pass through the units (see Fig. 5). This initial production of smaller drops with approximately the same shear 'settings' is due to the improved PS unit design. The inclusion of a second pass resulted in a small shift in the overall size distribution, with a reduction in average droplet size from 7.3 μm and 10.7 μm (at 25 ml/min and 50 ml/min, respectively) to 6.6 μm and 8.3 μm, respectively (Table 6). The impact of multiple passes using this setup (Setup 2) was therefore less pronounced than that observed using the previous SSHE/PS arrangement (Setup 1).

It is also worth noting that the average droplet sizes achieved using Setup 2, are similar to those reported earlier in Setup 1 but for higher residence times; either after a single/double pass at a lower flow rate (12 ml/min; see Table 2) or after multiple passes at the same flow rate (25 ml/min; see Table 3). However, the same does not apply with respect to span values, as Setup 1 can only deliver emulsions of a similarly narrow size distribution (to Setup 2) when operating at the lowest flow rate (12 ml/min). Increasing the residence time by repeated introduction of the emulsions through the shear environment generated by Setup 1 at higher flow rates, can somewhat reduce the level of droplet size variability (high span values) delivered upon the first passage, but cannot fully deliver the magnitude of droplet uniformity achieved by Setup 2.

3.3.2. The effect of the magnitude of applied shear

The effect of the level of shear applied by Setup 2 onto the produced W/O emulsions was studied by varying the rotation speed setting in the SSHE/PS units to 500, 1250 and 2000 rpm, while maintaining a flow rate of 25 ml/min and a cooling jacket temperature of 5°C. The droplet size distributions of all formed W/O emulsions are presented in Fig. 6A and D, while the calculated average droplet size diameters ($D_{3,2}$) and span values for each system are provided in Table 7.

The data shows that increasing levels of applied shear result in a decrease in droplet size, as the increased energy supplied by the rotating components of the SSHE and PS units promote further droplet break-up.

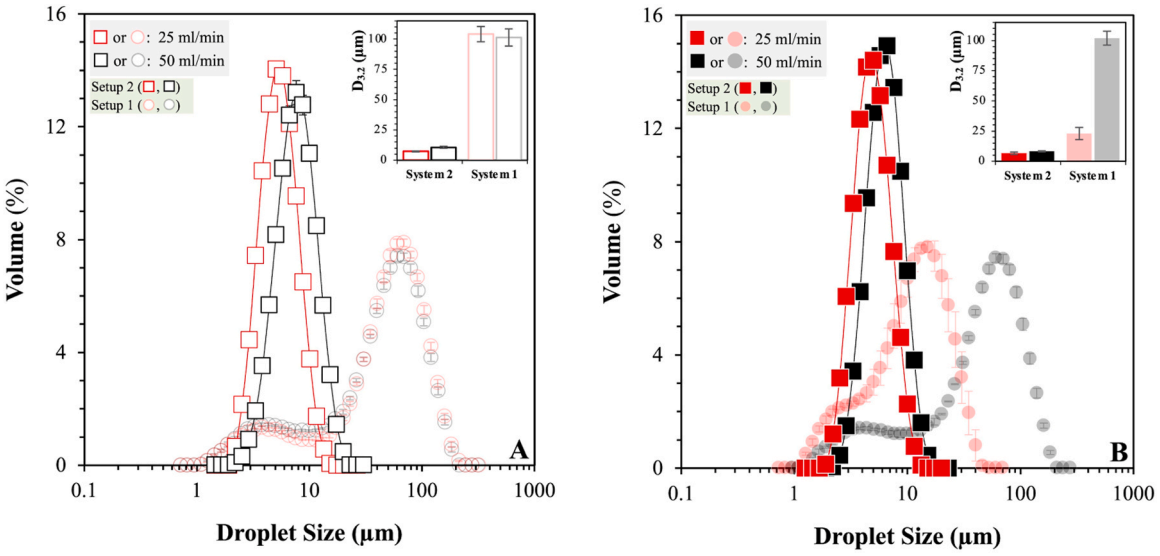

Fig. 5. Droplet size distributions of NaCl-containing (1 M in the aqueous dispersed phase) 30/70 W/O emulsions stabilised by a 1.75% (or 2.5% in the continuous phase) mono/triglyceride mixture (a 1:4 ratio of Dimodan and Tribehenin), as a function of flow rate and number of passes through the Setup 2 SSHE/PS units (o), operating at 1250 rpm and 5°C cooling; (A) single and (B) double pass data, respectively. Size distribution data for Setup 1 SSHE/PS units, operating at the same processing conditions, are also presented for comparison (o).

Table 6
Average droplet sizes (D3,2) and span values of NaCl-containing (1 M in the aqueous dispersed phase) 30/70 W/O emulsions stabilised by a 1.75% (or 2.5% in the continuous phase) mono/triglyceride mixture (a 1:4 ratio of Dimodan and Tribehenin), as a function of flow rate and number of passes through either the Setup 1 or Setup 2 SSHE/PS units; both operating at 1250 rpm and 5°C cooling.

		Setup 1		Setup 2	
	Flow Rate (ml/min)	$D_{3,2} \pm$ SD (μm)	span	$D_{3,2} \pm$ SD (μm)	span
Pass 1	25	104.1 ± 6.3	2.08	7.3 ± 0.1	1.01
	50	101.3 ± 7.0	2.16	10.7 ± 1.0	1.08
Pass 2	25	23.0 ± 5.0	1.92	6.6 ± 0.2	0.98
	50	101.9 ± 5.8	2.19	8.3 ± 0.2	0.95

As the likelihood of coalescence during processing increases with a reducing droplet size (at a fixed volume of dispersed phase, this increases the number of droplets in the system which in turn enhances the frequency of collision between them), it is also suggested that extending the level of shear also serves to facilitate better transport of the formed lipid crystals to the newly formed emulsion interfaces. A second pass through Setup 2 (regardless of the rotation speed setting used) does not appear to further reduce the droplet size, with both average droplet sizes and span values (compared to pass 1) remaining practically unchanged. It is therefore clear that W/O emulsions of practically the smallest size are already achieved by only a single passage through the processing environment in Setup 2. It is interesting to note that at the same flow rate (25 ml/min) and cooling temperature (5°C), W/O emulsions produced by Setup 2 at the lowest tested rotation speed (500 rpm) have droplet sizes that are more or less equivalent to those produced by Setup 1 at a higher level of applied shear (rotation speed of 1250 rpm) and after 5 processing passes (Table 3); even then however, the polydispersity (span value) of the former (Setup 2) is still lower (Table 7).

The salt release from W/O emulsions prepared with Setup 2 under a range of applied shears (rotation speeds) is shown in Fig. 6B and E. There is a sudden structure failure resulting in an abrupt (but not full) salt release for the single pass emulsion produced at 1250 rpm and the double pass emulsion formed at 2000 rpm; leading to an overall NaCl release of ~41% and ~9%, respectively. In addition to the magnitude, the onset of the observed NaCl burst is different between the two systems, taking place after 40 days of storage for the single pass emulsion formed at 1250 rpm and after 62 days for the double pass emulsion formed at 2000 rpm. However, for both systems the pronounced period of salt discharge is of similar duration (10–15 days) and is (in both cases) followed by practically no further NaCl release to the end of the 100-day testing period. This suggests that the lipid shells of a proportion of the droplet population were compromised during production. During release experimentation, placing these systems within a pure water sink creates an osmotic pressure gradient that eventually fully disrupts any such shell defects, leading to the full discharge of their saline content.

Considering the release performance from the emulsions produced by Setup 2 prior to the points of failure discussed above, the rotation speed (and thus magnitude of shear) in the SSHE/PS units appears to influence the capacity of the structures to regulate salt discharge. Higher rotational speeds seem to result in W/O emulsions with lipid shells that are more effective in terms of hindering salt release; however this is more pronounced as rotational speed is changed from 500 to 1250 rpm, rather than when it is then further increased from 1250 to 2000 rpm (Fig. 6B). Nonetheless, a second passage through Setup 2 does not seem to have any significant effect on salt release for any of the systems produced at the rotational speeds tested here (Fig. 6E). This observation contrasts the salt response behaviour exhibited by W/O emulsions produced by Setup 1, where a second processing pass at a rotational speed of 1250 rpm (Fig. 3B) depresses NaCl release. This differentiation in behaviour serves to further highlight the importance of shear uniformity in the PS unit of the used processing setup, not only in terms of reducing the droplet size of the produced emulsions (without repetition of the processing stages), but also in terms of providing a more robust lipid shell around them. It is clear that the use of the improved PS geometry in Setup 2 (resulting in the removal of the stagnant flow regions in its predecessor) also leads to lower salt release levels when compared to the Setup 1 units under similar processing conditions (Fig. 7).

Analysis of the calculated interfacial rate constants as a function of applied rotation speed leads to similar conclusions (Table 7). The increase in the magnitude of shear by moving to higher rotation speeds does lead to a decrease in the value of k_1, but the effect is modest. Carrying out a second processing step also results in some improvement (reduction in k_1), however this is practically non-existent at the highest rotation speed (2000 rpm) and certainly much less subdued to that exhibited by structures produced using Setup 1 at equivalent processing conditions (see Table 3). Specifically in terms of equivalent processing

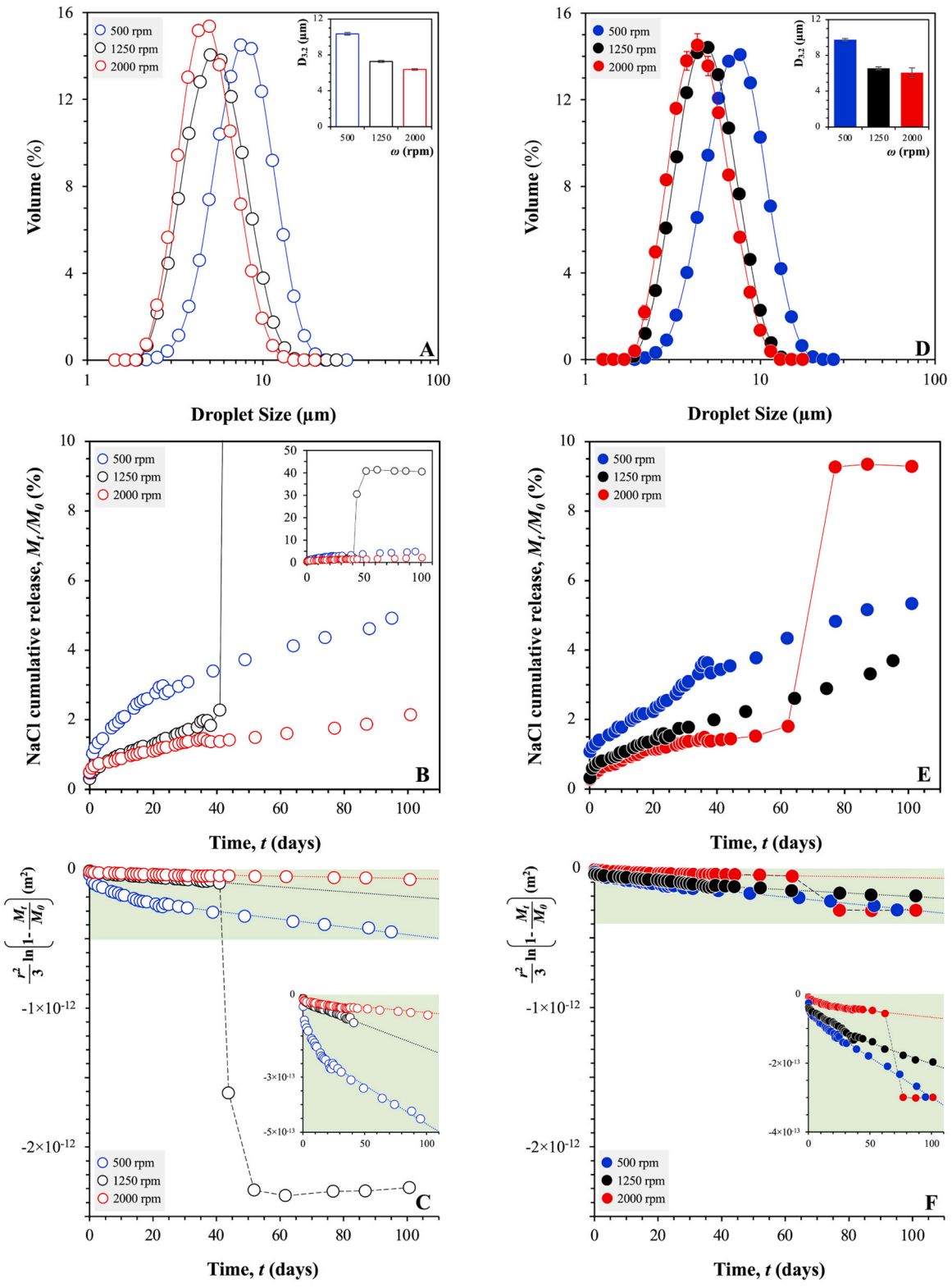

Fig. 6. A & D: Droplet size distributions of NaCl-containing (1 M in the aqueous dispersed phase) 30/70 W/O emulsions stabilised by a 1.75% (or 2.5% in the continuous phase) mono/triglyceride mixture (a 1:4 ratio of Dimodan and Tribehenin), as a function of rotation speed (applied shear) and number of passes through the SSHE/PS units (Setup 2), operating at 25 ml/min and 5°C cooling; (A) single and (D) double pass data. B & E: NaCl cumulative release (%) from W/O emulsions (detail as above) as a function of rotation speed and number of passes through the SSHE/PS units (detail as above); (B) single and (E) double pass data. C & F: First order fits to eq. (Berton-Carabin and Schroën, 2015) of data (for times $t \geq 10$ days) for the NaCl cumulative release from W/O emulsions (detail as above) as a function of rotation speed and number of passes through the SSHE/PS units (detail as above); (C) single and (F) double pass data. The graph areas of the inset plots in C and F are equivalent to the shaded areas in the main graphs.

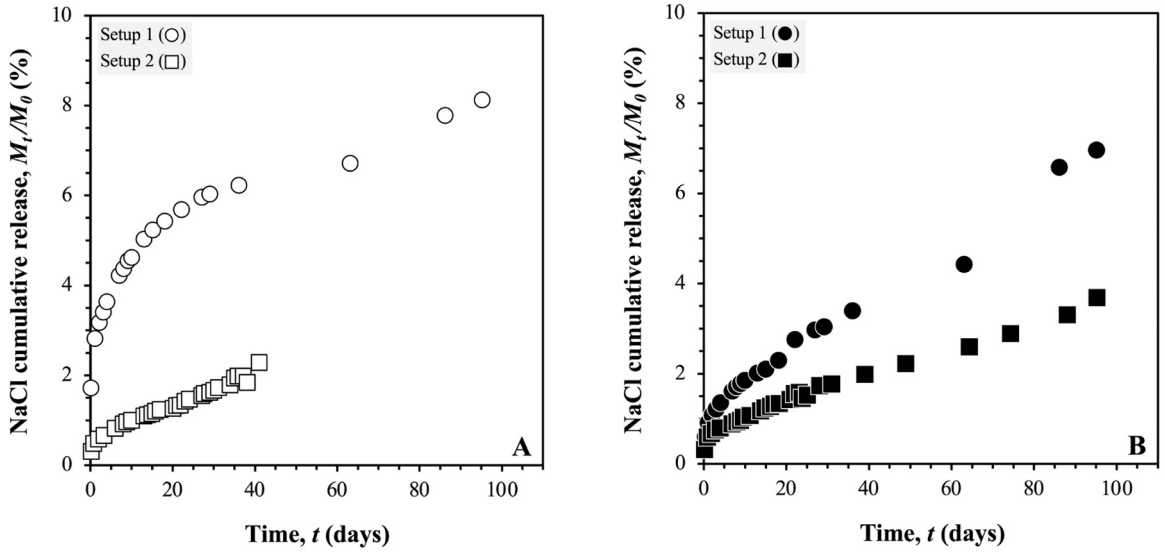

Fig. 7. Salt release (%) from NaCl-containing (1 M in the aqueous dispersed phase) 30/70 W/O emulsions stabilised by a 1.75% (or 2.5% in the continuous phase) mono/triglyceride mixture (a 1:4 ratio of Dimodan and Tribehenin), produced by either Setup 2 (O) or Setup 1 (O), both operating at 25 ml/min, 5°C cooling and 1250 rpm; (A) single and (B) double pass data.

Table 7
Average droplet sizes (D3,2) and span values of NaCl-containing (1 M in the aqueous dispersed phase) 30/70 W/O emulsions stabilised by a 1.75% (or 2.5% in the continuous phase) mono/triglyceride mixture (a 1:4 ratio of Dimodan and Tribehenin), as a function of rotation speed (applied shear) and number of passes through the SSHE/PS units (Setup 2), operating at 25 ml/min and 5°C cooling. Interfacial rate constants (k1) calculated by fitting the NaCl release from each of the tested W/O emulsions (see above) to Eq. (Berton-Carabin and Schroën, 2015), are also provided; SD: Standard Deviation.

	Rotational Speed (rpm)	$D_{3,2} \pm$ SD (μm)	span	$k_1 \pm$ SD $\times 10^{-3}$ (nm^2/s)	R^2
Pass 1	500	10.4 ± 0.1	0.96	32.4 ± 2.3	0.983
	1250	7.3 ± 0.1	1.01	19.8 ± 2.0	0.960
	2000	6.4 ± 0.1	0.93	4.7 ± 0.5	0.944
Pass 2	500	9.8 ± 0.1	1.01	26.9 ± 2.1	0.991
	1250	6.6 ± 0.2	0.98	14.3 ± 1.8	0.958
	2000	6.1 ± 0.5	0.99	4.3 ± 1.5	0.808

conditions (25 ml/min, 5°C cooling and 1250 rpm), lipid shells formed around emulsion droplets produced by Setup 1 require at least 5 processing steps (passes) to provide interfacial rate constants that are close to those delivered in W/O systems produced by Setup 1 in just one pass; 15.4×10^{-3} and 19.8×10^{-3} nm^2/s, respectively. Even then, there is a higher initial discharge of salt from systems provided by Setup 1 after 5 passes (compared to those obtained by Setup 2 after a single pass), suggesting that the much higher residence time associated with the former has jeopardised to some extent the integrity of the lipid shells around a higher proportion of emulsion droplets.

4. Conclusions

Fat crystal 'shell' stabilised water-in-oil emulsions produced via a scraped surface heat exchanger and pin stirrer (SSHE/PS) processing setup, were shown to be effective in regulating the slow release of NaCl entrapped within their water droplets. This work clearly demonstrates that the SSHE/PS processing conditions employed play a crucial role in determining the droplet sizes produced, the integrity of the interfacial lipid shells formed, and the salt release profiles achieved.

Emulsion droplet size is reduced by prolonging the residence time of the formulation in the SSHE/PS units (lower flow rates and/or repeated passes through the processing environment in the units), and ensuring it (the formulation) is exposed to a relatively uniform shear environment (by eliminating stagnant flow regions, particularly in the PS). Prolonging SSHE/PS residence time greatly enhances the integrity of the formed lipid shells and further suppresses salt release, only if accompanied by a droplet size reduction, as the latter promotes the build-up of additional crystalline matter around the emulsion droplets. Achieving shear uniformity results in more robust lipid shells and lower salt expulsion; processing setups of inferior shear uniformity (e.g. those with stagnant flow zones) can deliver emulsions with the same (salt retention/delivery) performance only at much higher residence times.

The used cooling temperature also affects the capacity of the formed lipid shell to hinder salt migration. Lower than optimum cooling temperatures (overcooling) will promote more rapid crystallisation phenomena and thus formation of larger lipid crystals, which in addition to leading to increased droplet sizes, also result in lipid shells with the lowest levels of interfacial hindrance. In this case, increasing residence times (while overcooling) will 'refine' the emulsions, lowering their droplet sizes and fortifying their lipid interfacial shells. In contrast, higher than optimum cooling temperatures (undercooling) will provide a reduced cooling potential which will result in a process that struggles to deliver the population of crystal species required for effective interfacial stabilisation. Here, longer residence times (while undercooling) will only further comprise the initially formed emulsions both in terms of their droplet size (and its uniformity) as well as the capacity to retain salt.

Overall, the current study offers significant direction in terms of the optimum processing requirements that are necessary to produce fat-continuous emulsion microstructures that can successfully regulate the release of NaCl. Interfacial rate constants for the lipid shells produced in this study ranged from 5.5 to 3593.2×10^{-3} nm^2/s and were significantly (up to three orders of magnitude) lower than those reported in literature for similar systems. This is a significant advancement in terms of salt retention, with the best performing emulsion structure produced here is reported to retain about 98% of its initial salt load over a period of 100 days. In terms of practical applications, it is envisaged that the technology presented here will allow the reformulation of appropriated classes of processed foods to create reduced-salt variants that are unchanged in terms of salt perception/"saltiness" and thus better placed for consumer acceptance. Future work needs to test this hypothesis and

thus will have to involving evaluating the applicability of this salt reduction microstructural strategy in real foods.

Declaration of Competing Interest

The authors declare the following financial interests/personal relationships which may be considered as potential competing interests: Fotis Spyropoulos reports financial support was provided by Engineering and Physical Sciences Research Council. Bruce Linter reports a relationship with PepsiCo International Ltd that includes: employment. Akash Beri reports a relationship with PepsiCo International Ltd that includes: employment. Fotis Spyropoulos is currently serving in an editorial capacity for the FBP journal If there are other authors, they declare that they have no known competing financial interests or personal relationships that could have appeared to influence the work reported in this paper. The views and opinions expressed in this manuscript are those of the authors and do not necessarily reflect the position or policy of PepsiCo, Inc.

Acknowledgements

The authors would like to thank the EPSRC (EP/J501670/1) and PepsiCo for contributions to the funding of this work. Thanks also go to Miss Lucie Villedieu for her study which has informed the methods used in this work. The confocal laser fluorescence microscope used in this research was obtained, through Birmingham Science City: Innovative Uses for Advanced Materials in the Modern World (West Midlands Centre for Advanced Materials Project 2), with support from Advantage West Midlands (AWM) and part funded by the European Regional Development Fund (ERDF).

References

K.A. Anderson, Margarine Processing Plants and Equipment, in: F. Shahadi (Ed.), Bailey's Industrial Oil and Fat Products, John Wiley and Sons, Hoboken, New Jersey, 2005, pp. 459-532.

Aveyard, R., Binks, B.P., Clint, J.H., 2003. Emulsions stabilised solely by colloidal particles. Adv. Colloid Interface Sci. 100–102 503–546.

V. di Bari, Large deformation and crystallisation properties of process optimised cocoa butter emulsions, Department of Chemical Engineering, The University of Birmingham, 2015.

di Bari, V., Norton, J.E., Norton, I.T., 2014. Effect of processing on the microstructural properties of water-in-cocoa butter emulsions. J. Food Eng. 122, 8–14.

Basso, R.C., Ribeiro, A.P.B., Masuchi, M.H., Gioielli, L.A., Gonçalves, L.A.G., Santos, A. Od, Cardoso, L.P., Grimaldi, R., 2010. Tripalmitin and monoacylglycerols as modifiers in the crystallisation of palm oil. Food Chem. 122, 1185–1192.

Berton-Carabin, C.C., Schroën, K., 2015. Pickering Emulsions for Food Applications: Background, Trends, and Challenges. Annu. Rev. Food Sci. Technol. 6, 263–297.

Dickinson, E., 2012. Use of nanoparticles and microparticles in the formation and stabilization of food emulsions. Trends Food Sci. Technol. 24, 4–12.

Dickinson, E., 2020. Advances in food emulsions and foams: reflections on research in the neo-Pickering era. Curr. Opin. Food Sci. 33, 52–60.

Dötsch, M., Busch, J., Batenburg, M., Liem, G., Tareilus, E., Mueller, R., Meijer, G., 2009. Strategies to reduce sodium consumption: a food industry perspective. Crit. Rev. Food Sci. Nutr. 49 (10), 841-851.

Douaire, M., di Bari, V., Norton, J.E., Sullo, A., Lillford, P., Norton, I.T., 2014. Fat crystallisation at oil–water interfaces. Adv. Colloid Interface Sci. 203, 1–10.

Dowding, P.J., Atkin, R., Vincent, B., Bouillot, P., 2005. Oil core/polymer shell microcapsules by internal phase separation from emulsion droplets. II: controlling the release profile of active molecules. Langmuir 21, 5278–5284.

S. Frasch-Melnik, Fat crystal-stabilised double emulsions, Department of Chemical Engineering, The University of Birmingham, 2011.

Frasch-Melnik, S., Norton, I.T., Spyropoulos, F., 2010. Fat-crystal stabilised W/O emulsions for controlled salt release. J. Food Eng. 98, 437–442.

A. Gabriele, Fluid Gels: Formation, Production and Lubrication, Department of Chemical Engineering, The University of Birmingham, 2011.

Ghosh, S., Rousseau, D., 2012. Triacylglycerol interfacial crystallization and shear structuring in water-in-oil emulsions. Cryst. Growth Des. 12, 4944–4954.

Guy, R.H., Hadgraft, J., Kellaway, I.W., Taylor, M.J., 1982. Calculations of drug release rates from particles. Int. J. Pharm. 11 (3), 199–207.

He, F.J., MacGregor, G.A., 2009. A comprehensive review on salt and health and current experience of worldwide salt reduction programmes. J. Hum. Hypertens. 23, 363–384.

Holm, K., Wendin, K., Hermansson, A.-M., 2009. Sweetness and texture perceptions in structured gelatin gels with embedded sugar rich domains. Food Hydrocoll. 23, 2388–2393.

Johansson, D., Bergenståhl, B., 1995. Sintering of fat crystal networks in oil during post-crystallization processes. J. Am. Oil Chem. Soc. 72, 911–920.

Krog, N., Larsson, K., 1992. Crystallization at interfaces in food emulsions – a general phenomenon. Lipid / Fett 94, 55–57.

Lucassen-Reynders, E.H., Tempel, M.V.D., 1963. Stabilization of water-in-oil emulsions by solid particles. J. Phys. Chem. 67, 731–734.

Meiselman, H.L., Halpern, B.P., 1973. Enhancement of taste intensity through pulsatile stimulation. Physiol. Behav. 11, 713–716.

Noort, M.W.J., Bult, J.H.F., Stieger, M., Hamer, R.J., 2010. Saltiness enhancement in bread by inhomogeneous spatial distribution of sodium chloride. J. Cereal Sci. 52, 378–386.

Norton, J.E., Fryer, P.J., 2012. Investigation of changes in formulation and processing parameters on the physical properties of cocoa butter emulsions. J. Food Eng. 113, 329–336.

Norton, J.E., Fryer, P.J., Parkinson, J., Cox, P.W., 2009. Development and characterisation of tempered cocoa butter emulsions containing up to 60% water. J. Food Eng. 95, 172–178.

Pickering, S.U., 1907. CXCVI.-Emulsions, journal of the chemical society. Transactions 91, 2001–2021.

Ramsden, W., 1903. Separation of solids in the surface-layers of solutions and 'suspensions' (observations on surface-membranes, bubbles, emulsions, and mechanical coagulation). – preliminary account. Proc. R. Soc. Lond. 72, 156–164.

Simovic, S., Prestidge, C.A., 2007. Nanoparticle layers controlling drug release from emulsions. Eur. J. Pharm. Biopharm. 67, 39–47.

Simovic, S., Prestidge, C.A., 2007. Nanoparticle layers controlling drug release from emulsions. Eur. J. Pharm. Biopharm. 67, 39–47.

Spyropoulos, F., Frasch-Melnik, S., Norton, I.T., 2011. W/O/W emulsions stabilized by fat crystals - their formulation, stability and ability to retain salt. Procedia Food Sci. 1, 1700–1708.

Spyropoulos, F., Clarke, C., Kurukji, D., Norton, I.T., Taylor, P., 2020. Emulsifiers of pickering-like characteristics at fluid interfaces: Impact on oil-in-water emulsion stability and interfacial transfer rate kinetics for the release of a hydrophobic model active. Colloids Surf. A: Physicochem. Eng. Asp. 607, 125413.

Washington, C., 1989. Evaluation of non-sink dialysis methods for the measurement of drug release from colloids: effects of drug partition. Int. J. Pharm. 56, 71–74.

Washington, C., Evans, K., 1995. Release rate measurements of model hydrophobic solutes from submicron triglyceride emulsions. J. Control. Release 33 (3), 383–390.

Yow, H.N., Routh, A.F., 2009. Release profiles of encapsulated actives from colloidosomes sintered for various durations. Langmuir 25 (1), 159–166.

Zafeiri, I., Smith, P., Norton, I.T., Spyropoulos, F., 2017. Fabrication, characterisation and stability of oil-in-water emulsions stabilised by solid lipid particles: the role of particle characteristics and emulsion microstructure upon Pickering functionality. Food Funct. 8, 2583–2591.